Brandner, Kay; Bauer, Michael; Seifert, Udo

Universal Coherence-Induced Power Losses of Quantum Heat Engines in Linear Response

Published in:
Physical Review Letters

DOI:
10.1103/PhysRevLett.119.170602

Published: 25/10/2017

Document Version
Publisher's PDF, also known as Version of record

Please cite the original version:
Brandner, K., Bauer, M., & Seifert, U. (2017). Universal Coherence-Induced Power Losses of Quantum Heat Engines in Linear Response. Physical Review Letters, 119(17), 1-7. [170602]. https://doi.org/10.1103/PhysRevLett.119.170602

Universal Coherence-Induced Power Losses of Quantum Heat Engines in Linear Response

Kay Brandner,[1] Michael Bauer,[2] and Udo Seifert[2]
[1]*Department of Applied Physics, Aalto University, 00076 Aalto, Finland*
[2]*II. Institut für Theoretische Physik, Universität Stuttgart, 70550 Stuttgart, Germany*

(Received 24 February 2017; revised manuscript received 21 August 2017; published 25 October 2017)

We identify a universal indicator for the impact of coherence on periodically driven quantum devices by dividing their power output into a classical contribution and one stemming solely from superpositions. Specializing to Lindblad dynamics and small driving amplitudes, we derive general upper bounds on both the coherent and the total power of cyclic heat engines. These constraints imply that, for sufficiently slow driving, coherence inevitably leads to power losses in the linear-response regime. We illustrate our theory by working out the experimentally relevant example of a single-qubit engine.

DOI: 10.1103/PhysRevLett.119.170602

Heat engines are devices that convert thermal energy into useful work. A Stirling motor, for example, uses the varying pressure of a periodically heated gas to produce mechanical motion (Fig. 1). Used by macroscopic engines for two centuries, this elementary operation principle has now been implemented on ever-smaller scales. Over the past decade, a series of experiments has shown that the working fluid of Stirling-type engines can be reduced to tiny objects such as a micrometer-sized silicon spring [1] or a single colloidal particle [2–5]. These efforts recently culminated in the realization of a single-atom heat engine [6,7]. Thus, the dimensions of the working fluid were further decreased by 4 orders of magnitude within only a few years. In light of this remarkable development, the challenge of even smaller engines operating on time and energy scales comparable to Planck's constant appears realistic for future experiments.

Quantum engines have access to a nonclassical mechanism of energy conversion that relies on the creation of coherence in their working fluid [8]; see Fig. 1. How does this additional freedom affect their performance? Having triggered substantial research efforts in recent years, this question constitutes one of the central problems in quantum thermodynamics; see, for example, Refs. [9–18]. However, the results now available are inconclusive. In fact, current evidence suggests that, depending on the specific setup, coherence can be either conducive [8,11,19–28] or detrimental [29–33].

Quantifying the role of coherence for a thermodynamic process requires a benchmark parameter that is sensitive to superpositions between the energy levels of the working medium. For operations involving nonselective measurements, several such figures were recently discussed; see, e.g., Refs. [34,35]. In this Letter, we put forward a universal coherence indicator for cyclic machines operating without external measurements. To this end, we describe the working fluid as a periodically driven N-level system with a time-dependent Hamiltonian H_t, which is embedded in a thermal environment. Provided that this reservoir is large, the system will settle to a periodic state ϱ_t after some transient time. The mean generated power per cycle of length $\mathcal{T}$ is then given by [31]

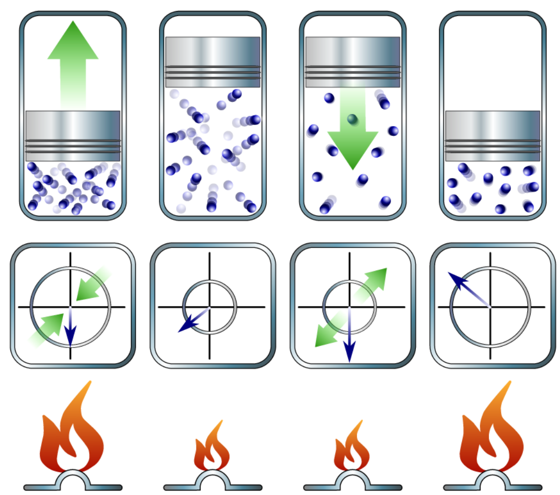

FIG. 1. Classical and quantum engines. (Upper panel) Macroscopic Stirling cycle. In the first stroke, power is extracted by expanding the hot working fluid. Decreasing the temperature at constant volume in the second stroke leads to a reduction of pressure before the gas is compressed again in the third stroke. The cycle is completed by isochorically returning to the initial temperature. (Lower panel) Quantum Stirling cycle. The working fluid consists of a two-level system, whose Bloch vector at the beginning of each stroke is shown in the four diagrams. The energy eigenstates lie on the vertical axis and the radius of the circle indicates the level splitting. Two distinct control operations are applied during the work strokes: the level splitting is changed and superpositions are created, i.e., the Bloch vector is rotated away from the vertical axis. In linear response, the energy content of these coherences cannot be regained by the controller; it is dissipated during the thermalization strokes, while the level population adapts to the temperature of the environment.

$$P = -\frac{1}{\mathcal{T}}\int_0^{\mathcal{T}} dt\mathrm{tr}\{\dot{H}_t\varrho_t\}. \tag{1}$$

Using the spectral decomposition

$$H_t \equiv \sum_n E_t^n |n_t\rangle\langle n_t| \tag{2}$$

of the time-dependent Hamiltonian, this quantity can be divided into two contributions corresponding to the different mechanisms of work extraction illustrated in Fig. 1. First, the classical power

$$P^d \equiv -\frac{1}{\mathcal{T}}\int_0^{\mathcal{T}} dt \sum_n \dot{E}_t^n \langle n_t|\varrho_t|n_t\rangle \tag{3}$$

generated by changing the energy levels of the working fluid depends only on the diagonal elements ϱ_t with respect to the instantaneous energy eigenstates. Second, the coherent power

$$P^c \equiv P - P^d = \frac{1}{\mathcal{T}}\int_0^{\mathcal{T}} dt \sum_n \langle \dot{n}_t|[H_t, \varrho_t]|n_t\rangle \tag{4}$$

arises from creating superpositions between these states [36]. Accordingly, P^c vanishes when ϱ_t commutes with H_t throughout the cycle or when the eigenvectors of H_t are time independent.

We note that the separation of the power operator $\dot{H}_t$ into a diagonal and an off-diagonal part has been discussed in the context of adiabatic processes [37] and for a specific model of a quantum Otto engine [38]. Here, we obtained the identifications (3) and (4) without making any assumptions on the time scale of the driving, the driving protocol or the system-reservoir coupling. In fact, they follow directly from the expression (1) for the total generated power, which can be regarded as a consequence of the first law applied to the compound system of working fluid and environment. Therefore, the coherent power (4) qualifies as a universal indicator for the impact of coherence on periodic power generation, which, besides heat engines, could also be applied to other types of devices such as feedback engines [12,23,39,40].

As a first key application of this concept, we will explore how coherence affects the power of slowly driven heat engines in linear response. Our analysis thereby builds on the well-established theory of open quantum systems [41,42] and a recently developed thermodynamic framework describing periodically driven systems [31,43], which has already proven very useful in the classical realm [44–47]. To describe a quantum heat engine, we augment the setup discussed so far with a heat source, which periodically injects thermal energy into the environment at a rate much slower than its internal relaxation time. The working fluid then effectively feels the time-dependent temperature

$$T_t \equiv T + f_t^q, \quad \text{with} \quad f_t^q \geq 0. \tag{5}$$

Work is extracted through a periodic driving field f_t^w, which couples linearly to the system degree of freedom G^w. The Hamiltonian H_t thus assumes the form

$$H_t \equiv H + f_t^w G^w. \tag{6}$$

For uniqueness, the field f_t^w is chosen to be dimensionless and with a vanishing average over one period $\mathcal{T}$.

Deriving constraints on the coherent power P^c requires us to further specify the dynamics of the working fluid. To this end, we first consider the equilibrium situation, i.e., $f_t^q = f_t^w = 0$. Assuming weak system-reservoir coupling and applying a coarse graining in time to wipe out memory effects and fast oscillating contributions to the state ϱ_t then yields the Markovian master equation

$$\partial_t\varrho_t = -\frac{i}{\hbar}[H, \varrho_t] + \mathsf{D}\varrho_t, \tag{7}$$

where the dissipator

$$\mathsf{D}X \equiv \sum_\sigma \frac{\gamma_\sigma}{2}([V_\sigma X, V_\sigma^\dagger] + [V_\sigma, XV_\sigma^\dagger]) \tag{8}$$

accounts for the effective influence of the thermal environment [41,42,48–50]. Here, $\hbar$ denotes Planck's constant and $\{\gamma_\sigma\}$ is a set of positive rates with corresponding Lindblad operators $\{V_\sigma\}$. Owing to microreversibility, these quantities are constrained by the quantum detailed balance relation, which can be expressed compactly in terms of the formal identity [48,51]

$$\mathsf{D}e^{-\beta H} = e^{-\beta H}\mathsf{D}^\dagger. \tag{9}$$

Here, $\beta \equiv 1/(k_B T)$, where k_B denotes Boltzmann's constant, and the adjoint dissipator is given by [42]

$$\mathsf{D}^\dagger X \equiv \sum_\sigma \frac{\gamma_\sigma}{2}(V_\sigma^\dagger[X, V_\sigma] + [V_\sigma^\dagger, X]V_\sigma). \tag{10}$$

In the adiabatic regime, where the driving is slow compared to the coarse-graining time scale used in the derivation of Eq. (7), finite driving can be included in this framework by allowing the rates and the Lindblad operators to be time dependent and replacing H and T with H_t and T_t, respectively, in Eqs. (7)–(10) [41]. Solving the resulting master equation with time-dependent generator by treating f_t^q and f_t^w as first-order perturbations then yields the explicit expressions [52]

$$P^d \equiv -\frac{1}{\mathcal{T}}\int_0^{\mathcal{T}} dt \int_0^\infty d\tau \dot{f}_t^w (\dot{C}_\tau^{dd} f_{t-\tau}^w + \dot{C}_\tau^{dq} f_{t-\tau}^q),$$
$$P^c \equiv -\frac{1}{\mathcal{T}}\int_0^{\mathcal{T}} dt \int_0^\infty d\tau \dot{f}_t^w \dot{C}_\tau^{cc} f_{t-\tau}^w \tag{11}$$

for the classical and the coherent power, respectively [53], in the following notation. We abbreviate with C_t^{ab} the Kubo correlation function [54]

$$C_t^{ab} \equiv \langle\!\langle \hat{G}_t^a, \hat{G}_0^b \rangle\!\rangle \equiv \int_0^\beta d\lambda (\langle \hat{G}_t^a e^{-\lambda H} \hat{G}_0^b e^{\lambda H} \rangle - \langle \hat{G}_t^a \rangle \langle \hat{G}_0^b \rangle), \quad (12)$$

where $t \geq 0$ and each of the indices a and b can assume the values d, c, q. Hats indicate Heisenberg-picture operators satisfying the adjoint master equation [42]

$$\partial_t \hat{X}_t = \frac{i}{\hbar}[H, \hat{X}_t] + \mathsf{D}^\dagger \hat{X}_t, \quad \text{with} \quad \hat{X}_0 = X. \quad (13)$$

Angular brackets denote the thermal average throughout, i.e., $\langle X \rangle \equiv \mathrm{tr}\{X e^{-\beta H}\}/\mathrm{tr}\{e^{-\beta H}\}$. Finally, we have defined the operator $G^q \equiv -H/T$ and split G^w into a diagonal and a coherent part,

$$G^d \equiv \sum_n |n\rangle\langle n|G^w|n\rangle\langle n| \quad \text{and} \quad G^c \equiv G^w - G^d, \quad (14)$$

where the vectors $|n\rangle$ correspond to the eigenstates of the unperturbed Hamiltonian H.

As a first key observation, we note that the expression (11) for P^c is independent of the temperature profile f_t^q. Thus, under linear-response and adiabatic-driving conditions, it is impossible to convert thermal energy provided by the heat source into positive power output via quantum coherence; rather, coherent power can be injected into the system only through mechanical driving. This constraint is captured quantitatively by the bound

$$P^c \leq -\frac{L_1^c \Omega^2}{\Omega^2 + L_2^c/L_1^c} F^w \leq 0, \quad (15)$$

which is saturated in the limit $\Omega \equiv 2\pi/\mathcal{T} \to 0$ and, formally, also for $\Omega \to \infty$; for the proof, see the Supplemental Material [55]. It involves the mean square amplitude $F^w \equiv (1/\mathcal{T}) \int_0^\mathcal{T} dt (f_t^w)^2$ of the driving field, and the Green-Kubo–type coefficients

$$L_j^c \equiv \int_0^\infty dt \langle\!\langle \hat{G}_t^{c(j)}, \hat{G}_0^{c(j)} \rangle\!\rangle \geq 0, \quad (16)$$

where the index j in brackets means a time derivative of respective order.

The bound (15) can be understood intuitively by identifying the parameter L_2^c/L_1^c as an estimator for the decoherence strength of the reservoir, i.e., the square of the mean rate, at which its influence destroys coherent superpositions between the energy levels of the working fluid. In the incoherent limit $L_2^c/L_1^c \gg \Omega^2$, the coherent power can approach zero due to frequent interactions with the environment constantly forcing the system into a state that is diagonal in the instantaneous energy eigenbasis. This behavior resembles the quantum Zeno effect, with the role of the observer played by the thermal reservoir [42]. If L_2^c/L_1^c is comparable to Ω^2, coherences are inevitably established in the working fluid at the price of injected coherent power. Accordingly, in the extreme case $L_2^c/L_1^c \ll \Omega^2$, the upper bound (15) reduces to $P^c \leq -L_1^c F^w$, its minimum with respect to Ω. Since this physical picture appears to be quite general, we assume that the coherent power is universally negative in linear response. It should, however, be noted that Eq. (15) strictly holds only if the driving is slow enough not to spoil the validity of the adiabatic master equation leading to Eq. (11). A quantitative analysis of the rapid-driving regime would therefore require a different dynamical description of the working fluid using, for example, the Floquet-Lindblad approach [56].

The coefficients (16) vanish if and only if $G^c = 0$, which means that the control variable G^w commutes with the unperturbed Hamiltonian H. Thus, according to Eq. (15), any nonclassical driving will inevitably reduce the net output $P = P^d + P^c$ of the engine. In fact, P is subject to the upper bound

$$P \leq \frac{L_1^q F^q}{4(1 + \psi_\Omega)}, \quad \text{with} \quad \psi_\Omega \equiv \frac{(L_1^c/L_1^d)\Omega^2}{\Omega^2 + L_2^c/L_1^c} \geq 0, \quad (17)$$

which is proven in the Supplemental Material [55]. For $a = d$ and $a = q$, the protocol-independent parameters L_j^a, which are reminiscent of linear transport coefficients, are thereby defined analogously to Eq. (16), with G^c replaced by G^d and G^q, respectively. Furthermore, $F^q \equiv (1/\mathcal{T}) \int_0^\mathcal{T} dt (f_t^q - \bar{f}^q)^2$, with $\bar{f}^q \equiv (1/\mathcal{T}) \int_0^\mathcal{T} dt f_t^q$ corresponding to the mean square magnitude of the local temperature variation induced by the heat source.

In the special case of purely coherent driving, $G^d = 0$, the coefficient L_1^d vanishes. The coherence parameter ψ_Ω, which provides a measure for the relative strength of coherent and classical driving, then diverges, and Eq. (17) reduces to $P \leq 0$. Consequently, in line with our analysis above, no cyclic engine relying only on coherent work extraction can properly operate in the linear-response regime. For $G^c = 0$, i.e., quasiclassical driving, ψ_Ω vanishes and the constraint (17) assumes its weakest form,

$$P \leq L_1^q F^q / 4. \quad (18)$$

This bound can be saturated if and only if

$$G^w = -\mu H/T \quad \text{and} \quad \mathsf{D}^\dagger H = -\lambda (H - \langle H \rangle) \quad (19)$$

for some real scalars μ and $\lambda > 0$ [55]. Thus, the field f_t^w has to couple to the free Hamiltonian H, and the energy correlations must decay exponentially with rate λ, i.e.,

$$\langle\!\langle \hat{H}_t, \hat{H}_0 \rangle\!\rangle = e^{-\lambda t} \langle\!\langle \hat{H}_0, \hat{H}_0 \rangle\!\rangle. \quad (20)$$

If these two requirements are fulfilled, the protocol for optimal power extraction is determined by the condition [55]

$$2\dot{f}_t^w = \lambda (f_t^q - \bar{f}^q)/\mu - \dot{f}_t^q/\mu, \quad (21)$$

which leads to $P = L_1^q F_q/4$ for any temperature profile f_t^q and for sufficiently short operation cycles [57]. Furthermore, using relation (20), the upper bound (18) can be expressed in a physically transparent form,

$$L_1^q = \lambda \frac{\langle H^2 \rangle - \langle H \rangle^2}{k_B T^3}. \tag{22}$$

Hence, the strength and the decay rate of the energy fluctuations in equilibrium essentially determine the maximum power of a cyclic N-level engine in the linear-response regime. A similar result was obtained only recently for classical engines [43,45].

We will now explore the quality of our bounds under practical conditions. To this end, we consider a two-level engine with the time-dependent Hamiltonian

$$H_t = \frac{\hbar\omega}{2}\sigma_z + \frac{\hbar\omega f_t^w}{2}(r\sigma_z + (1-r)\sigma_x). \tag{23}$$

Here, $\sigma_{x,y,z}$ are the usual Pauli matrices, and the dimensionless parameter $0 \le r \le 1$ determines the relative weight of the classical and coherent parts, $G^d = r(\hbar\omega/2)\sigma_z$ and $G^c = (1-r)(\hbar\omega/2)\sigma_x$, of the control variable G^w. The corresponding equilibrium dissipator (8) involves two Lindblad operators, $V_\pm = (\sigma_x \pm i\sigma_y)/2$, acting at the rates $\gamma_\pm \equiv \gamma e^{\mp\kappa}$, respectively, where $\kappa \equiv \hbar\omega\beta/2$. This setup lies within the range of forthcoming experiments using a superconducting qubit to realize the system and ultrafast electron thermometers for calorimetric work measurements [58–60]. Its coherent and total power are subject to the bounds

$$P^c \le -\frac{\hbar\omega\lambda}{2} r^2 g\psi_\Omega F^w \quad \text{and} \quad P \le \frac{\hbar\omega\lambda}{8}\frac{g}{1+\psi_\Omega}\frac{F^q}{T^2},$$
$$\text{with} \quad \psi_\Omega = \frac{(1-r)^2}{r^2}\frac{\sinh 2\kappa}{4\kappa}\frac{\Omega^2}{\Omega^2+\omega^2+\lambda^2/4}, \tag{24}$$

$g \equiv \kappa/\cosh^2\kappa$, and $\lambda \equiv 2\gamma\cosh\kappa$, which follow from Eqs. (15) and (17) [55].

To assess the quality of these constraints, we choose a temperature profile f_t^q that mimics the Stirling cycle illustrated in Fig. 1 and a work protocol satisfying

$$2\dot{f}_t^w = -\Omega(f_t^q - \bar{f}^q)/T + \dot{f}_t^q/T, \tag{25}$$

both of which are shown in Fig. 2. This choice renders the amplitude and shape of f_t^w independent of the cycle frequency Ω. In Fig. 2, the resulting coherent power is plotted as a function of Ω/λ for $r = 1/2$. If the level splitting ω is significantly smaller than the dissipation rate λ, it decays monotonically while closely following its upper bound (24). With an increasing ω, a resonant dip emerges close to $\Omega = \omega$. This feature is not reproduced by our bound, which is, however, still saturated in the limit $\Omega/\lambda \to 0$ and, formally, also for $\Omega/\lambda \to \infty$. For $r = 1$, the coherent power vanishes and the two conditions (19) are fulfilled with $\mu = -T$. The total power P plotted in Fig. 2 then reaches its upper bound (24) at $\Omega = \lambda$, i.e., when the work protocol (25) satisfies the maximum-power condition (21). As r varies from 1 to 0, the total power decreases more and more due to coherence-induced losses, and the bound (24) lies well above the actual value of P. This result underlines our general conclusion that coherence has a purely detrimental effect on the output of cyclic heat engines operated slowly and in linear response.

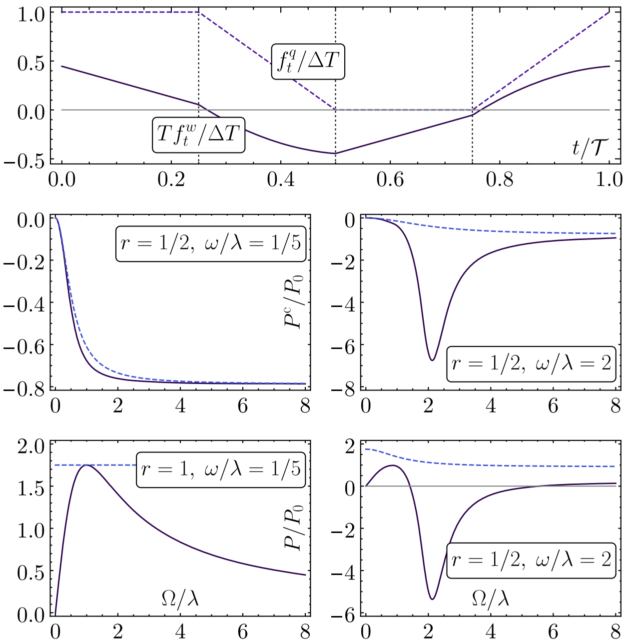

FIG. 2. Single-qubit engine. (Upper panel) The temperature profile f_t^q (dashed line) consists of two isothermal steps at temperatures $T + \Delta T$ and T connected by linear slopes. The work protocol f_t^w (solid line) is determined by the condition (25). (Lower panels) Coherent and total power (solid lines) in units of $P_0 \equiv (\hbar\omega\lambda/2)(\Delta T/T)^2 10^{-2}$ as functions of the rescaled frequency Ω/λ. The bounds (24) are shown for comparison (dashed lines). The plots in the left column show that our bounds (15) and (17) can be practically saturated for $\omega/\lambda \ll 1$. For $\omega/\lambda > 1$, coherence-induced features (resonant dips) appear in both P^c and P; see the right column. For all plots, we have set $\kappa \equiv 1$.

In the nonlinear regime, coherence can indeed be beneficial since strong driving makes it possible to extract work from superpositions before they are destroyed by the thermal reservoir. This mechanism is exploited by continuous quantum engines like the three-level maser [61,62], which produce purely nonclassical power. It also underlies the coherence-induced power enhancement recently observed for stroke engines in the limit of short cycle times [8]. Capturing this effect quantitatively in terms of coherent power would require us to further develop our approach by including higher orders in the driving fields. In a broader perspective, this path could lead to a universal classification of features enabling an increase of power through coherence, e.g., squeezed reservoirs [11] or collective behavior [18,27], and features leading to coherence-induced power losses like quantum friction; the last phenomenon was observed earlier in various models describing the working fluid as an interacting spin system [29,30,38,63,64].

We conclude by stressing that our key expressions (3) and (4) are valid for an arbitrary driving strength and speed and for any type of system-reservoir coupling. The coherent power (4) can therefore be used as a universal performance benchmark across various different types of cyclic machines, including rapidly driven [26,65–69] and strongly coupled [70–75] engines. Finally, it might even be possible to extend this concept to thermoelectric nano devices, a second class of quantum engines, which has recently attracted remarkable interest [76–90]. Eventually, our approach could thus lead to a comprehensive understanding of the role of quantum effects for one of the most fundamental thermodynamic operations: the conversion of heat into power.

K. B. acknowledges financial support from the Academy of Finland (Contract No. 296073) and is affiliated with the Centre of Quantum Engineering. K. B. thanks J. P. Pekola, M. Campisi, and R. Fazio for the insightful discussions.

[1] P. G. Steeneken, K. Le Phan, M. J. Goossens, G. E. J. Koops, G. J. A. M. Brom, C. van der Avoort, and J. T. M. van Beek, Piezoresistive heat engine and refrigerator, Nat. Phys. **7**, 354 (2011).
[2] V. Blickle and C. Bechinger, Realization of a micrometer-sized stochastic heat engine, Nat. Phys. **8**, 143 (2011).
[3] I. A. Martínez, É. Roldán, L. Dinis, D. Petrov, and R. A. Rica, Adiabatic Processes Realized with a Trapped Brownian Particle, Phys. Rev. Lett. **114**, 120601 (2015).
[4] I. A. Martínez, É. Roldán, L. Dinis, D. Petrov, J. M. R. Parrondo, and R. A. Rica, Brownian Carnot engine, Nat. Phys. **12**, 67 (2015).
[5] S. Krishnamurthy, S. Ghosh, D. Chatterji, R. Ganapathy, and A. K. Sood, A micrometer-sized heat engine operating between bacterial reservoirs, Nat. Phys. **12**, 1134 (2016).
[6] J. Roßnagel, S. T. Dawkins, K. N. Tolazzi, O. Abah, E. Lutz, F. Schmidt-Kaler, and K. Singer, A single-atom heat engine, Science **352**, 325 (2016).
[7] O. Abah, J. Roßnagel, G. Jacob, S. Deffner, F. Schmidt-Kaler, K. Singer, and E. Lutz, Single-Ion Heat Engine at Maximum Power, Phys. Rev. Lett. **109**, 203006 (2012).
[8] R. Uzdin, A. Levy, and R. Kosloff, Equivalence of Quantum Heat Machines, and Quantum-Thermodynamic Signatures, Phys. Rev. X **5**, 031044 (2015).
[9] H. T. Quan, Yu-xi Liu, C. P. Sun, and F. Nori, Quantum thermodynamic cycles and quantum heat engines, Phys. Rev. E **76**, 031105 (2007).
[10] K. Funo, Y. Watanabe, and M. Ueda, Thermodynamic work gain from entanglement, Phys. Rev. A **88**, 052319 (2013).
[11] J. Roßnagel, O. Abah, F. Schmidt-Kaler, K. Singer, and E. Lutz, Nanoscale Heat Engine beyond the Carnot Limit, Phys. Rev. Lett. **112**, 030602 (2014).
[12] J. P. Pekola, Towards quantum thermodynamics in electronic circuits, Nat. Phys. **11**, 118 (2015).
[13] H. Zhou, J. Thingna, P. Hänggi, J.-S. Wang, and B. Li, Boosting thermoelectric efficiency using time-dependent control, Sci. Rep. **5**, 14870 (2015).
[14] M. Lostaglio, K. Korzekwa, D. Jennings, and T. Rudolph, Quantum Coherence, Time-Translation Symmetry, and Thermodynamics, Phys. Rev. X **5**, 021001 (2015).
[15] P. Ćwikliński, M. Studziński, M. Horodecki, and J. Oppenheim, Limitations on the Evolution of Quantum Coherences: Towards Fully Quantum Second Laws of Thermodynamics, Phys. Rev. Lett. **115**, 210403 (2015).
[16] B. Gardas and S. Deffner, Thermodynamic universality of quantum Carnot engines, Phys. Rev. E **92**, 042126 (2015).
[17] H. Tasaki, Quantum Statistical Mechanical Derivation of the Second Law of Thermodynamics: A Hybrid Setting Approach, Phys. Rev. Lett. **116**, 170402 (2016).
[18] J. Jaramillo, M. Beau, and A. Del Campo, Quantum supremacy of many-particle thermal machines, New J. Phys. **18**, 075019 (2016).
[19] M. O. Scully, K. R. Chapin, K. E. Dorfman, M. B. Kim, and A. Svidzinsky, Quantum heat engine power can be increased by noise-induced coherence, Proc. Natl. Acad. Sci. U.S.A. **108**, 15097 (2011).
[20] S. Abe and S. Okuyama, Role of the superposition principle for enhancing the efficiency of the quantum-mechanical Carnot engine, Phys. Rev. E **85**, 011104 (2012).
[21] L. A. Correa, J. P. Palao, D. Alonso, and G. Adesso, Quantum-enhanced absorption refrigerators, Sci. Rep. **4**, 3949 (2014).
[22] J. M. Horowitz and K. Jacobs, Quantum effects improve the energy efficiency of feedback control, Phys. Rev. E **89**, 042134 (2014).
[23] K. Brandner, M. Bauer, M. T. Schmid, and U. Seifert, Coherence-enhanced efficiency of feedback-driven quantum engines, New J. Phys. **17**, 065006 (2015).
[24] M. T. Mitchison, M. P. Woods, J. Prior, and M. Huber, Coherence-assisted single-shot cooling by quantum absorption refrigerators, New J. Phys. **17**, 115013 (2015).
[25] J. B. Brask and N. Brunner, Small quantum absorption refrigerator in the transient regime: Time scales, enhanced cooling, and entanglement, Phys. Rev. E **92**, 062101 (2015).
[26] D. Gelbwaser-Klimovsky, W. Niedenzu, P. Brumer, and G. Kurizki, Power enhancement of heat engines via correlated thermalization in a three-level working fluid, Sci. Rep. **5**, 14413 (2015).
[27] R. Uzdin, Coherence-Induced Reversibility and Collective Operation of Quantum Heat Machines via Coherence Recycling, Phys. Rev. Applied **6**, 024004 (2016).
[28] G. Watanabe, B. P. Venkatesh, P. Talkner, and A. del Campo, Quantum Performance of Thermal Machines Over Many Cycles, Phys. Rev. Lett. **118**, 050601 (2017).
[29] T. Feldmann and R. Kosloff, Quantum four-stroke heat engine: Thermodynamic observables in a model with intrinsic friction, Phys. Rev. E **68**, 016101 (2003).

[30] T. Feldmann and R. Kosloff, Characteristics of the limit cycle of a reciprocating quantum heat engine, Phys. Rev. E **70**, 046110 (2004).

[31] K. Brandner and U. Seifert, Periodic thermodynamics of open quantum systems, Phys. Rev. E **93**, 062134 (2016).

[32] A. Roulet, S. Nimmrichter, J. M. Arrazola, S. Seah, and V. Scarani, Autonomous rotor heat engine, Phys. Rev. E **95**, 062131 (2017).

[33] B. Karimi and J. P. Pekola, Otto refrigerator based on a superconducting qubit—Classical and quantum performance, Phys. Rev. B **94**, 184503 (2016).

[34] P. Kammerlander and J. Anders, Coherence and measurement in quantum thermodynamics, Sci. Rep. **6**, 22174 (2016).

[35] C. Elouard, D. A. Herrera-Martí, M. Clusel, and A. Auffèves, The role of quantum measurement in stochastic thermodynamics, npj Quantum Inf. **3**, 9 (2017).

[36] To make these definitions unique, we understand that the time-dependent energy eigenvalues are arranged in increasing order, i.e., $E_t^0 \leq E_t^1 \leq \cdots \leq E_t^N$ for all cases where $t \in \mathbb{R}$, where we assume that N is finite for simplicity. Furthermore, we note that the expressions (3) and (4) are unaltered if the instantaneous energy eigenstates are multiplied by arbitrary time-dependent phase factors.

[37] H. T. Quan, P. Zhang, and C. P. Sun, Quantum heat engine with multilevel quantum systems, Phys. Rev. E **72**, 056110 (2005).

[38] T. Feldmann and R. Kosloff, Quantum lubrication: Suppression of friction in a first-principles four-stroke heat engine, Phys. Rev. E **73**, 025107(R) (2006).

[39] C. Elouard, D. Herrera-Martí, B. Huard, and A. Auffèves, Extracting Work from Quantum Measurement in Maxwell's Demon Engines, Phys. Rev. Lett. **118**, 260603 (2017).

[40] N. Cottet, S. Jezouin, L. Bretheau, P. Campagne-Ibarcq, Q. Ficheux, J. Anders, A. Auffèves, R. Azouit, P. Rouchon, and B. Huard, Observing a quantum Maxwell demon at work, Proc. Natl. Acad. Sci. U.S.A. **114**, 7561 (2017).

[41] R. Alicki, The quantum open system as a model of the heat engine, J. Phys. A **12**, L103 (1979).

[42] H.-P. Breuer and F. Petruccione, *The Theory of Open Quantum Systems*, 1st ed. (Clarendon Press, Oxford, 2006).

[43] K. Brandner, K. Saito, and U. Seifert, Thermodynamics of Micro- and Nano-Systems Driven by Periodic Temperature Variations, Phys. Rev. X **5**, 031019 (2015).

[44] K. Proesmans and C. Van den Broeck, Onsager Coefficients in Periodically Driven Systems, Phys. Rev. Lett. **115**, 090601 (2015).

[45] M. Bauer, K. Brandner, and U. Seifert, Optimal performance of periodically driven, stochastic heat engines under limited control, Phys. Rev. E **93**, 042112 (2016).

[46] K. Proesmans, Y. Dreher, M. Gavrilov, J. Bechhoefer, and C. Van den Broeck, Brownian Duet: A Novel Tale of Thermodynamic Efficiency, Phys. Rev. X **6**, 041010 (2016).

[47] K. Proesmans, B. Cleuren, and C. Van den Broeck, Power-Efficiency-Dissipation Relations in Linear Thermodynamics, Phys. Rev. Lett. **116**, 220601 (2016).

[48] H. Spohn and J. L. Lebowitz, Irreversible thermodynamics for quantum systems weakly coupled to thermal reservoirs, Adv. Chem. Phys. **38**, 109 (1978).

[49] D. A. Lidar, Z. Bihary, and K. B. Whaley, From completely positive maps to the quantum Markovian semigroup master equation, Chem. Phys. **268**, 35 (2001).

[50] A. Levy, R. Alicki, and R. Kosloff, Quantum refrigerators and the third law of thermodynamics, Phys. Rev. E **85**, 061126 (2012).

[51] R. Alicki, On the detailed balance condition for non-Hamiltonian systems, Rep. Math. Phys. **10**, 249 (1976).

[52] To obtain Eq. (11) from Eqs. (3) and (4), standard linear-response theory is applied. This derivation exploits the fact that, due to the detailed balance relation (9), the space of all system operators commuting with the unperturbed Hamiltonian H is invariant under the action of the superoperators D and $\mathsf{D}^\dagger$; for details, see Ref. [31].

[53] The detailed balance relation (9) implies that the set of Lindblad operators $\{V_\sigma\}$ is self-adjoint; see Ref. [51] and A. Kossakowski, A. Frigerio, V. Gorini, and M. Verri, Quantum detailed balance and KMS condition, Commun. Math. Phys. **57**, 97 (1977)]; Additionally, we assume here that this set is irreducible such that $X = 1$ is the only solution of $\mathsf{D}^\dagger X = 0$ [H. Spohn, An algebraic condition for the approach to equilibrium of an open N-level system, Lett. Math. Phys. **2**, 33 (1977)]. Under this condition, the improper integrals showing up in Eq. (11) are well defined [31].

[54] R. Kubo, M. Toda, and N. Hashitsume, *Statistical Physics II—Nonequilibrium Statistical Mechanics*, 2nd ed. (Springer, Tokyo, 1998).

[55] See Supplemental Material at http://link.aps.org/supplemental/10.1103/PhysRevLett.119.170602 for derivations of the bounds (15), (17), (24) and the condition (21).

[56] The Floquet-Lindblad equation can be derived in a similar way as the adiabatic master equation [41] used in this Letter; see, for example, Ref. [50] and R. Alicki, D. A. Lidar, and P. Zanardi, Internal consistency of fault-tolerant quantum error correction in light of rigorous derivations of the quantum Markovian limit, Phys. Rev. A **73**, 052311 (2006)]. However, in the Floquet-Lindblad approach, the coarse-graining time scale is larger than the period of the external modulation. Thus, by carrying out the coarse graining, the driving is effectively averaged in time. Combining this method with the concept of coherent power would therefore require us to adapt the expressions (3) and (4) to the time coarse-grained picture.

[57] For long cycles, the reduced temperature profile $f_t^q - f^q$ would oscillate slowly and thus be either positive or negative over substantial time ranges. Consequently, integrating Eq. (21) would yield a driving protocol f_t^w with a large amplitude, which violates the linear-response condition underlying the derivations leading to Eqs. (18) and (21).

[58] S. Gasparinetti, K. L. Viisanen, O.-P. Saira, T. Faivre, M. Arzeo, M. Meschke, and J. P. Pekola, Fast Electron Thermometry for Ultrasensitive Calorimetric Detection, Phys. Rev. Applied **3**, 014007 (2015).

[59] K. L. Viisanen, S. Suomela, S. Gasparinetti, O.-P. Saira, J. Ankerhold, and J. P. Pekola, Incomplete measurement of work in a dissipative two level system, New J. Phys. **17**, 055014 (2015).

[60] J. P. Pekola, P. Solinas, A. Shnirman, and D. V. Averin, Calorimetric measurement of work in a quantum system, New J. Phys. **15**, 115006 (2013).

[61] H. E. D. Scovil and E. O. Schulz-DuBois, Three Level Masers as Heat Engines, Phys. Rev. Lett. **2**, 262 (1959).
[62] E. Geva and R. Kosloff, Three-level quantum amplifier as a heat engine: A study in finite-time thermodynamics, Phys. Rev. E **49**, 3903 (1994).
[63] R. Kosloff and T. Feldmann, Discrete four-stroke quantum heat engine exploring the origin of friction, Phys. Rev. E **65**, 055102(R) (2002).
[64] T. Feldmann and R. Kosloff, Short time cycles of purely quantum refrigerators, Phys. Rev. E **85**, 051114 (2012).
[65] G. B. Cuetara, A. Engel, and M. Esposito, Stochastic thermodynamics of rapidly driven systems, New J. Phys. **17**, 055002 (2015).
[66] R. Alicki and D. Gelbwaser-Klimovsky, Non-equilibrium quantum heat machines, New J. Phys. **17**, 115012 (2015).
[67] D. Gelbwaser-Klimovsky and G. Kurizki, Heat-machine control by quantum-state preparation: From quantum engines to refrigerators, Phys. Rev. E **90**, 022102 (2014).
[68] D. Gelbwaser-Klimovsky, R. Alicki, and G. Kurizki, Minimal universal quantum heat machine, Phys. Rev. E **87**, 012140 (2013).
[69] M. Kolář, D. Gelbwaser-Klimovsky, R. Alicki, and G. Kurizki, Quantum Bath Refrigeration towards Absolute Zero: Challenging the Unattainability Principle, Phys. Rev. Lett. **109**, 090601 (2012).
[70] M. F. Ludovico, J. S. Lim, M. Moskalets, L. Arrachea, and D. Sánchez, Dynamical energy transfer in ac-driven quantum systems, Phys. Rev. B **89**, 161306(R) (2014).
[71] M. Esposito, M. A. Ochoa, and M. Galperin, Nature of heat in strongly coupled open quantum systems, Phys. Rev. B **92**, 235440 (2015).
[72] R. Uzdin, A. Levy, and R. Kosloff, Quantum heat machines equivalence, work extraction beyond Markovianity, and strong coupling via heat exchangers, Entropy **18**, 124 (2016).
[73] P. Strasberg, G. Schaller, N. Lambert, and T. Brandes, Nonequilibrium thermodynamics in the strong coupling and non-Markovian regime based on a reaction coordinate mapping, New J. Phys. **18**, 073007 (2016).
[74] M. Carrega, P. Solinas, M. Sassetti, and U. Weiss, Energy Exchange in Driven Open Quantum Systems at Strong Coupling, Phys. Rev. Lett. **116**, 240403 (2016).
[75] D. Newman, F. Mintert, and A. Nazir, Performance of a quantum heat engine at strong reservoir coupling, Phys. Rev. E **95**, 032139 (2017).
[76] T. E. Humphrey and H. Linke, Quantum, cyclic, and particle-exchange heat engines, Physica (Amsterdam) **29E**, 390 (2005).
[77] K. Brandner, K. Saito, and U. Seifert, Strong Bounds on Onsager Coefficients and Efficiency for Three-Terminal Thermoelectric Transport in a Magnetic Field, Phys. Rev. Lett. **110**, 070603 (2013).
[78] K. Brandner and U. Seifert, Multi-terminal thermoelectric transport in a magnetic field: Bounds on Onsager coefficients and efficiency, New J. Phys. **15**, 105003 (2013).
[79] D. Venturelli, R. Fazio, and V. Giovannetti, Minimal Self-Contained Quantum Refrigeration Machine Based on Four Quantum Dots, Phys. Rev. Lett. **110**, 256801 (2013).
[80] R. S. Whitney, Most Efficient Quantum Thermoelectric at Finite Power Output, Phys. Rev. Lett. **112**, 130601 (2014).
[81] J. Matthews, F. Battista, D. Sánchez, P. Samuelsson, and H. Linke, Experimental verification of reciprocity relations in quantum thermoelectric transport, Phys. Rev. B **90**, 165428 (2014).
[82] C. Bergenfeldt, P. Samuelsson, B. Sothmann, C. Flindt, and M. Büttiker, Hybrid Microwave-Cavity Heat Engine, Phys. Rev. Lett. **112**, 076803 (2014).
[83] P. P. Hofer, J. R. Souquet, and A. A. Clerk, Quantum heat engine based on photon-assisted Cooper pair tunneling, Phys. Rev. B **93**, 041418(R) (2016).
[84] R. Sánchez, B. Sothmann, and A. N. Jordan, Chiral Thermoelectrics with Quantum Hall Edge States, Phys. Rev. Lett. **114**, 146801 (2015).
[85] K. Brandner and U. Seifert, Bound on thermoelectric power in a magnetic field within linear response, Phys. Rev. E **91**, 012121 (2015).
[86] K. Yamamoto and N. Hatano, Thermodynamics of the mesoscopic thermoelectric heat engine beyond the linear-response regime, Phys. Rev. E **92**, 042165 (2015).
[87] K. Yamamoto, O. Entin-Wohlman, A. Aharony, and N. Hatano, Efficiency bounds on thermoelectric transport in magnetic fields: The role of inelastic processes, Phys. Rev. B **94**, 121402(R) (2016).
[88] G. Marchegiani, P. Virtanen, F. Giazotto, and M. Campisi, Self-Oscillating Josephson Quantum Heat Engine, Phys. Rev. Applied **6**, 054014 (2016).
[89] P. Samuelsson, S. Kheradsoud, and B. Sothmann, Optimal Quantum Interference Thermoelectric Heat Engine with Edge States, Phys. Rev. Lett. **118**, 256801 (2017).
[90] Y. Zheng, P. Hänggi, and D. Poletti, Occurrence of discontinuities in the performance of finite-time quantum Otto cycles, Phys. Rev. E **94**, 012137 (2016).